Development 136, 699 (2009) doi:10.1242/dev.034264

Prox1 maintains muscle structure and growth in the developing heart

Catherine A. Risebro, Richelle G. Searles, Athalie A. D. Melville, Elisabeth Ehler, Nipurna Jina, Sonia Shah, Jacky Pallas, Mike Hubank, Miriam Dillard, Natasha L. Harvey, Robert J. Schwartz, Kenneth R. Chien, Guillermo Oliver and Paul R. Riley

There was an error published in the ePress version of *Development* **136**, 495-505 on the 17th December 2008.

The acknowledgements should have mentioned funding from the National Institutes of Health and the American Lebanese Syrian Associated Charities. The corrected acknowledgements section appears in full below. The final online and print versions are correct.

The authors apologise to readers for this mistake.

We thank K. Venner for technical assistance with electron microscopy, A. Cook for advice on E18.5 heart analysis, C. Shang for advice on the ChIP protocol, D. Kelberman for advice on the EMSA protocol, and D. Fürst (titin and α-actinin) and T. Obinata (MyBP-C) for antibodies. This work was funded by the British Heart Foundation, the Medical Research Council, and by R01-HL073402 (G.O.) from the National Institutes of Health and by the American Lebanese Syrian Associated Charities (ALSAC). Deposited in PMC for release after 12 months.

Development 136, 495-505 (2009) doi:10.1242/dev.030007

Prox1 maintains muscle structure and growth in the developing heart

Catherine A. Risebro[1], Richelle G. Searles[1], Athalie A. D. Melville[1], Elisabeth Ehler[2], Nipurna Jina[3], Sonia Shah[4], Jacky Pallas[4], Mike Hubank[3], Miriam Dillard[5], Natasha L. Harvey[6], Robert J. Schwartz[7], Kenneth R. Chien[8,9], Guillermo Oliver[5] and Paul R. Riley[1,*]

Impaired cardiac muscle growth and aberrant myocyte arrangement underlie congenital heart disease and cardiomyopathy. We show that cardiac-specific inactivation of the murine homeobox transcription factor Prox1 results in the disruption of expression and localisation of sarcomeric proteins, gross myofibril disarray and growth-retarded hearts. Furthermore, we demonstrate that Prox1 is required for direct transcriptional regulation of the genes encoding the structural proteins α-actinin, N-RAP and zyxin, which collectively function to maintain an actin–α-actinin interaction as the fundamental association of the sarcomere. Aspects of abnormal heart development and the manifestation of a subset of muscular-based disease have previously been attributed to mutations in key structural proteins. Our study reveals an essential requirement for direct transcriptional regulation of sarcomere integrity, in the context of enabling foetal cardiomyocyte hypertrophy, maintenance of contractile function and progression towards inherited or acquired myopathic disease.

KEY WORDS: Prox1, Mouse, Heart development, Myocardium, Sarcomere, Hypertrophy, Myopathy, N-RAP (Nrap), Zyxin

INTRODUCTION

Cardiac muscle integrity and function is dependent upon the maintenance of a rhythmically contracting meshwork of myofibrils, the basic structural and functional unit of which is known as the sarcomere. Sarcomeres are multi-protein complexes comprising interlacing myosin (thick) and actin (thin) filaments bordered by Z-discs. Several proteins important for the stability of sarcomeric structure are found in the Z-disc, which not only has a structural role for cross-linking thin filaments and transmitting contractile force, but also provides a vital interface for signal transduction and biomechanical sensing (Frank et al., 2006; Pyle and Solaro, 2004).

There is an absolute requirement for cardiac function during embryogenesis in mammals and as such the sarcomeric components are expressed very early in development and are correctly localised in the myofibrils by the time the linear heart tube begins to contract (Ehler et al., 1999). As development progresses, the heart increases in mass not only by cardiomyocyte hyperplasia, but also through a recently recognised foetal phase of physiological hypertrophy (Hirschy et al., 2006), a process that is dependent upon myofibril disassembly, reassembly (Ahuja et al., 2004) and elongation (Hirschy et al., 2006).

[1]Molecular Medicine Unit, UCL Institute of Child Health, London WC1N 1EH, UK. [2]The Randall Centre of Cell and Molecular Biophysics and The Cardiovascular Division, King's College, London SE1 1UL, UK. [3]Molecular Haematology and Cancer Biology Unit, UCL Institute of Child Health, London WC1N 1EH, UK. [4]Bloomsbury Centre for Bioinformatics, Department of Computer Science, University College London, Gower Street, London WC1E 6BT, UK. [5]Department of Genetics and Tumor Cell Biology, St Jude Children's Research Hospital, 332 N. Lauderdale, Memphis, TN 38105, USA. [6]Division of Haematology, The Hanson Institute, Adelaide, South Australia 5000, Australia. [7]Institute of Biosciences and Technology, Texas A&M University Health Science Center, Houston, TX 77030, USA. [8]Massachusetts General Hospital Cardiovascular Research Center, Boston, MA 02114, USA. [9]Department of Cell Biology, Harvard Medical School, and the Harvard Stem Cell Institute, Cambridge, MA 02138, USA.

*Author for correspondence (e-mail: p.riley@ich.ucl.ac.uk)

Accepted 21 November 2008

Despite insight into the morphogenetic events that accompany myofibrillogenesis and hypertrophic growth, very little is known about the precise regulation of these processes during development. Furthermore, the importance of appropriate assembly and maintenance of the myofibrillar apparatus is underscored by the fact that defects in the terminal differentiation and arrangement of contractile protein filaments are associated with a number of cardiac myopathies (Engel, 1999; Gregorio and Antin, 2000; Seidman and Seidman, 2001).

The homeobox transcription factor Prox1 is essential for murine lymphatic, hepatocyte, retinal and pancreatic development (Dyer et al., 2003; Harvey et al., 2005; Sosa-Pineda et al., 2000; Wigle and Oliver, 1999). Multiple lines of evidence suggest a role for Prox1 during cardiac morphogenesis. *Prox1* is expressed in the developing heart (Oliver et al., 1993; Rodriguez-Niedenfuhr et al., 2001; Tomarev et al., 1996; Wigle and Oliver, 1999) and embryos deficient in Prox1 die at ~E14.5, a critical time point when lethality often results from grossly reduced cardiac performance (Dyson et al., 1995). Moreover, in a specific genetic background, a proportion of *Prox1*-heterozygote mice fail to survive and become cyanotic soon after birth (Harvey et al., 2005), a phenotype that is consistent with impaired blood circulation and heart defects.

Here we reveal how Prox1 functions transcriptionally upstream of sarcomere assembly, myofibril organisation and foetal cardiomyocyte growth. We provide evidence that Prox1 activity is required for the normal expression and localisation of multiple sarcomeric components and that it directly regulates the genes encoding α-actinin, N-RAP (nebulin-related anchoring protein, Nrap) and zyxin, which are essential structural proteins required for stabilising actin within the thin filaments and ultimately for establishing cardiomyocyte elongation and coordinated muscle contraction. These results, therefore, provide important insight into the molecular mechanisms that govern the ultrastructure and growth of cardiac muscle during development and highlight how transcriptional misregulation of myofibril assembly may underlie cardiac hypotrophy and myopathic disease.

MATERIALS AND METHODS

Mouse strains and histology

The mouse strains used have been described previously: *Prox1*-null (Wigle et al., 1999), *Prox1*^{loxP} (Harvey et al., 2005), Nkx2.5CreKI (Moses et al., 2001) and MLC2vCreKI (Chen et al., 1998). *Prox1*$^{loxP/loxP}$ mice were crossed with Nkx2.5CreKI;*Prox1*^{loxP} or MLC2vCreKI;*Prox1*^{loxP} to generate Nkx2.5CreKI;*Prox1*$^{loxP/loxP}$ (*Prox1*^{Nkx}) or MLC2vCreKI;*Prox1*$^{loxP/loxP}$ (*Prox1*^{MLC}) embryos, respectively. Embryos and hearts were dissected in PBS, fixed in 4% paraformaldehyde (PFA), dehydrated, embedded in paraffin and sectioned at 15 μm. Sections were stained with Haematoxylin and Eosin.

Immunohistochemistry and TUNEL assays

Embryos were treated as above and sectioned at 10 μm. Immunohistochemistry was performed using anti-Prox1 (Reliatech) and anti-phosphohistone H3 (Upstate) antibodies, developed using a standard streptavidin-HRP method and counterstained with Haematoxylin. Terminal deoxynucleotidyl transferase biotin-dUTP nick end labelling (TUNEL) assays were performed according to the manufacturer's protocols (Promega).

Immunofluorescence and confocal microscopy

E10.5-14.5 whole-mount hearts were dissected in PBS and fixed overnight in 4% PFA. E18.5 hearts were dissected, embedded in paraffin and sectioned as above. Immunofluorescence and confocal microscopy were performed as described previously (Ehler et al., 1999). Samples were analysed on a Zeiss LSM 510 confocal microscope equipped with argon and helium neon lasers using a 63×/1.4 lens. Image processing was performed using Zeiss software and Photoshop (Adobe). Cell outlines were traced on sections (blinded to genotype), using ImageJ (http://rsb.info.nih.gov/ij) to assist in assessing cell shape and calculating cell area as indicators of foetal hypertrophy.

Antibodies

The following antibodies were used: sarcomeric α-actinin (clone EA-53; Sigma), β-catenin, vinculin and smooth muscle α-actin (clone 1A4; Sigma), cardiac α-actin (Progen), titin (T12; gift of Prof. D. Fürst, Institut für Zellbiologie, Universität Bonn, Germany), desmin (clone D33; Dako), MHC (A4.1025; DSHB), cardiac MyBP-C (gift of Prof. T. Obinata, Department of Biology, Chiba University, Japan), CD31 (Pecam1; BD Pharmingen), Prox1 (Reliatech) and Gapdh (Chemicon). For western blots, rabbit anti-sarcomeric α-actinin antibody was used (gift of Prof. D. Fürst).

Transmission electron microscopy

E13.5/E18.5 hearts were dissected and fixed in 3% glutaraldehyde (EM grade, Agar Scientific), 0.1 M sodium cacodylate, 5 mM $CaCl_2$ (pH 7.4). Hearts were processed in a Lynx automated tissue processor (Australian Biomedical) and embedded in resin. All sectioning was performed on a Reichert Ultracut S ultramicrotome. Sections were imaged using a Philips CM 10 transmission electron microscope and images collected using Kodak Megaview II and SIS Keenview digital imaging systems and SIS software. Four *Prox1*^{Nkx} and four control hearts were examined for each stage.

Western blotting

E13.5 heart lysates were prepared in RIPA buffer. Western blotting was performed using standard methods. Scanning densitometry was performed and signal quantified using Scion Image (Scion Corporation) and ImageJ.

Quantitative real-time (qRT) PCR analysis

mRNA was isolated from E12.5 hearts using the Micro FastTrack 2.0 Kit (Invitrogen) according to the manufacturer's instructions. Reverse transcription was performed using Superscript III reverse transcriptase (Invitrogen) according to the manufacturer's instructions. qRT-PCR analysis was performed on an ABI 7000 Sequence Detector (Applied Biosystems) using SYBR Green (Quantitect SYBR Green PCR Kit, Qiagen). Data were normalised to *Hprt1* expression and analysed using DART-PCR (Peirson et al., 2003). *P*-values were obtained using Student's *t*-test (n=9). Primers for qRT-PCR (Table 1) were obtained from Primer Bank (http://pga.mgh.harvard.edu/primerbank) or designed using Primer Express (version 2.0, Applied Biosystems).

RNA in situ hybridisation on embryonic sections

E13.5 embryos were fixed in 4% PFA, embedded in paraffin and sectioned at 15 μm. RNA in situ hybridisation on sections was performed as previously described (Moorman et al., 2001), using a digoxigenin-labelled antisense riboprobe specific for *Nppa* (Kuo et al., 1997).

ChIP-on-chip

E12.5 hearts were dissected in PBS containing 0.3% Triton X-100 and cross-linked for 3 hours at room temperature in 1.8% formaldehyde, homogenised in lysis buffer and sonicated. Sixty micrograms of chromatin lysate was used per immunoprecipitation with 10 μg anti-Prox1 antibody (Reliatech) in ChIP dilution buffer at 4°C overnight. A no-antibody 'immunoprecipitation' was performed as a control. Immune complexes were pulled down with Protein A/G beads, washed, resuspended in TE (10 mM Tris, 5 mM EDTA, pH 8.0), the cross-links reversed overnight at 65°C and the DNA purified. DNA (10 ng) was blunt-ended and unidirectional adapters were ligated overnight at 16°C. Adapter-ligated DNA was amplified by PCR. Experimental conditions, buffer composition, adapter sequences and PCR conditions are available on request. ChIP and no-antibody samples were checked by qRT-PCR for enrichment of a positive control, *Fgfr3* (a previously identified in vitro target of Prox1) (Shin et al., 2006), and against a negative control, *Cyp7a1* (Qin et al., 2004). Amplified DNA (7.5 μg) was fragmented and end labelled using the GeneChip WT Double-Stranded DNA Terminal Labelling Kit, hybridised to GeneChip Mouse Promoter 1.0R Arrays, and then stained using the GeneChip Hybridisation, Wash and Stain Kit (all Affymetrix). ChIP data were analysed

Table 1. Primer sequences (5′ to 3′) for PCR

qRT-PCR

Gene	Forward	Reverse	Amplicon (bp)
Actn2	TGGCACCCAGATCGAGAAC	GTGGAACCGCATTTTTCCCC	121
Actc1	CTGGATTCTGGCGATGGTGTA	CGGACAATTTCACGTTCAGCA	173
Ttn	CCAGGCCCTCCAAACAACC	CCATTCACCAACACTCACATCAC	141
Myh7	ACTGTCAACACTAAGAGGGTCA	TTGGATGATTTGATCTTCCAGGG	114
Des	GTGGATGCAGCCACTCTAGC	TTAGCCGCGATGGTCTCATAC	218
Prox1	GAAGGGCTATCACCCAATCA	TGAACCACTTGATGAGCTGC	142
Hprt	TCAGTCAACGGGGGACATAAA	GGGGCTGTACTGCTTAACCAG	142
Mybpc3	CAGGGAAGAAACCAGTGTCAG	GCTGCCAAACCATACTTGTCATT	166
Nppa	TTCCTCGTCTTGGCCTTTTG	CCTCATCTTCTACCGGCATCTTC	136
Nrap	CTCTAGGTGTGGCTATGGGGT	AGTACGGCTTTTTCTGGTGAC	143
Zyx	CAGGGAGAAAGTGTGCAGTATT	TCGTTCTTGGTCATGTCGTCC	75

PCR to confirm ChIP

Enhancer region	Forward	Reverse	Amplicon (bp)
Actn2	CCTCTTCTTCAACCGAACCA	CCAACTCTGCTTTTTCCCAG	129
Nrap	CAAGGATTGCTGAAGGGAAA	CACCTCCATGTCTCCTTGGT	295
Zyx	CATGCTAGGCAGGCACTGTA	AGATATGAGAAGCCCCCACC	273

using CisGenome (v1.0_beta; http://www.biostat.jhsph.edu/~hji/cisgenome/index.htm). Three independent ChIP and no-antibody control reactions were performed. Standard PCR to confirm ChIP of the enhancer elements was carried out using the primers listed in Table 1.

EMSAs

Electrophoretic mobility shift assays (EMSAs) were carried out as described previously (Angelo et al., 2000). Briefly, in vitro translated Prox1, or nuclear extracts from mouse P19Cl6 cells (Habara-Ohkubo, 1996) transfected with Flag-Prox1, were incubated with ^{32}P-labelled oligonucleotide in binding buffer at room temperature for 30 minutes. Overlapping 60 bp oligonucleotides, which spanned the entire Prox1-binding elements of *Actn2*, *Nrap* and *Zyx* as identified by ChIP-on-chip, were used in preliminary binding reactions to narrow down each element to within a single 60 bp oligonucleotide (sequences highlighted in red in Fig. S9 in the supplementary material). Unlabelled oligonucleotide (10-fold excess) was used in the competition binding assays. Anti-Flag (M2; Sigma; 4.6 μg) was used to supershift bound Prox1 in the transfected P19Cl6 cell extracts. Each binding reaction was run on an 8% polyacrylamide gel, which was dried and subjected to autoradiography.

Reporter transactivation assays

P19CL6 cells were maintained in standard P19 culture conditions (McBurney et al., 1982). Transfections were carried out using Effectene reagent as described previously (Hill and Riley, 2004). Briefly, duplicate wells of P19CL6 cells were transfected with a reporter in which luciferase was located downstream of putative Prox1-binding elements from *Actn2*, *Nrap* or *Zyx*, and a chick α-cardiac actin minimal promoter (Hill and Riley, 2004), either with or without pcDNA3-Prox1 (250 ng) and a β-actin–β-galactosidase (β-gal) expressing plasmid to normalise luciferase activity for transfection efficiency. Luciferase and β-gal activity were assayed 48 hours post-transfection as described (Hill and Riley, 2004).

RESULTS

Prox1 is expressed in the embryonic heart

In the first instance we characterised Prox1 expression during murine embryonic heart development. Immunostaining revealed that Prox1 is expressed throughout the entire myocardium of the atria, ventricles and outflow tract from ~E10.5 (Fig. 1). At E12.5 and E14.5, Prox1 expression was notable in the interventricular septum and myocardium (Fig. 1B-E), but was excluded from the smooth muscle of the outflow tract (not shown). Furthermore, Prox1 was expressed in the outer endocardial layer of the atrioventricular endocardial cushion leaflets (Fig. 1E,F) and the mitral valve leaflets (Fig. 1F,H), but was absent from cushion mesenchyme (Fig. 1F,G). Confocal analysis confirmed the predicted nuclear localisation of Prox1 in atrial and ventricular myocytes (see Fig. S1A-D in the supplementary material).

Heart development is abnormal in *Prox1*-null mice

Mice that are homozygous null for *Prox1* die between E14.5 and E15 (Wigle and Oliver, 1999). The cause of lethality in *Prox1*-null embryos has not been determined. To address whether loss of cardiac expression of *Prox1* is a potential contributing factor, we initially examined surviving post-natal day 5 (P5) *Prox1*-heterozygous mice and observed, at a gross anatomical level, that the hearts were reduced in size (by an average of 30%) as compared with those of wild-type littermate controls (see Fig. S2A in the supplementary material). Histological analysis revealed a range of cardiac anomalies including hypoplastic ventricular walls, loss of muscle striation, a disorganised interventricular septum and abnormally persistent muscle surrounding the aorta (see Fig. S2B,D in the supplementary material). Analysis of *Prox1*-null embryos at E13.5 and E14.5 revealed that mutant hearts were significantly smaller (up to 50%) than those of wild-type littermates (see Fig. S2E,F in the supplementary material) and, consistent with the phenotype in the P5 heterozygotes, we observed myocardial disarray, including a disrupted interventricular septum (see Fig. S2G,H in the supplementary material).

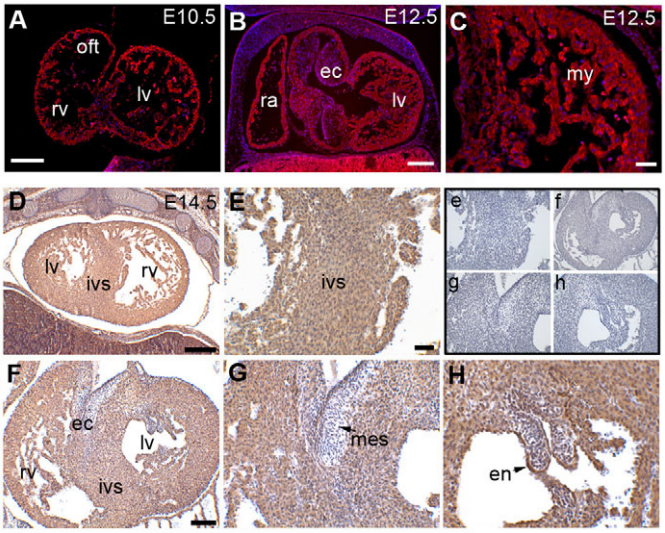

Fig. 1. Prox1 is expressed in the myocardium of the developing mouse heart. (**A-C**) Immunofluorescence on E10.5 (A) and E12.5 (B,C) frontal sections using an antibody for Prox1. Prox1 is expressed throughout the myocardium of the presumptive left and right ventricles and outflow tract at E10.5 (A) and is localised to both atrial and ventricular myocardium at E12.5 (B,C). (**D-H**) Immunohistochemistry on E14.5 frontal sections illustrates continued expression of Prox1 throughout the entire myocardium (D), in the interventricular septum (E), the endocardium of the atrioventricular canal endocardial cushions (F,G) and mitral valve leaflets (F,H). Prox1 is absent from cushion mesenchyme (F,G). Panels e-h show the no-primary-antibody controls for the corresponding panels E-H. lv, left ventricle; rv, right ventricle; ivs, interventricular septum; ec, endocardial cushion; en, endocardium; mes, mesenchyme; oft; outflow tract; ra, right atrium; my, myocardium. Scale bars: 50 μm in A,B,D; 25 μm in F; 10 μm in C,E,G,H.

Prox1 is an essential regulator of heart development

Conventional *Prox1*-null embryos have a lymphatic phenotype arising from defects in endothelial cell budding as early as E11.5 (Wigle and Oliver, 1999), which may adversely affect cardiovascular development. To confirm a primary role for Prox1 in the developing heart, we generated a cardiac-specific knockout of *Prox1* by crossing a conditional homozygous floxed *Prox1* strain (*Prox1*$^{loxP/loxP}$) (Harvey et al., 2005) with two cardiac-expressing Cre strains: Nkx2.5^{Cre}KI (designated *Prox1*^{Nkx}), which directs expression of Cre recombinase throughout the majority of cardiomyocytes from E7.5 (Moses et al., 2001); and MLC2v^{Cre}KI (designated *Prox1*^{MLC}), in which Cre is expressed specifically in ventricular cardiomyocytes from E8.75 (Chen et al., 1998). The two Cre strains were employed, therefore, to target *Prox1* globally throughout the entire myocardium and in a subpopulation of ventricular myocardium, thus acting as respective internal controls for a cardiomyocyte-specific loss of Prox1 function.

Prox1 protein levels in *Prox1*^{Nkx} and *Prox1*^{MLC} E13.5 hearts were analysed by western blot on whole heart lysates, followed by densitometry. This confirmed a ~3-fold reduction in Prox1 protein levels in the cardiac-specific knockout hearts as compared with littermate control hearts (*Prox1*^{loxP} or Cre allele only) (Fig. 2A).

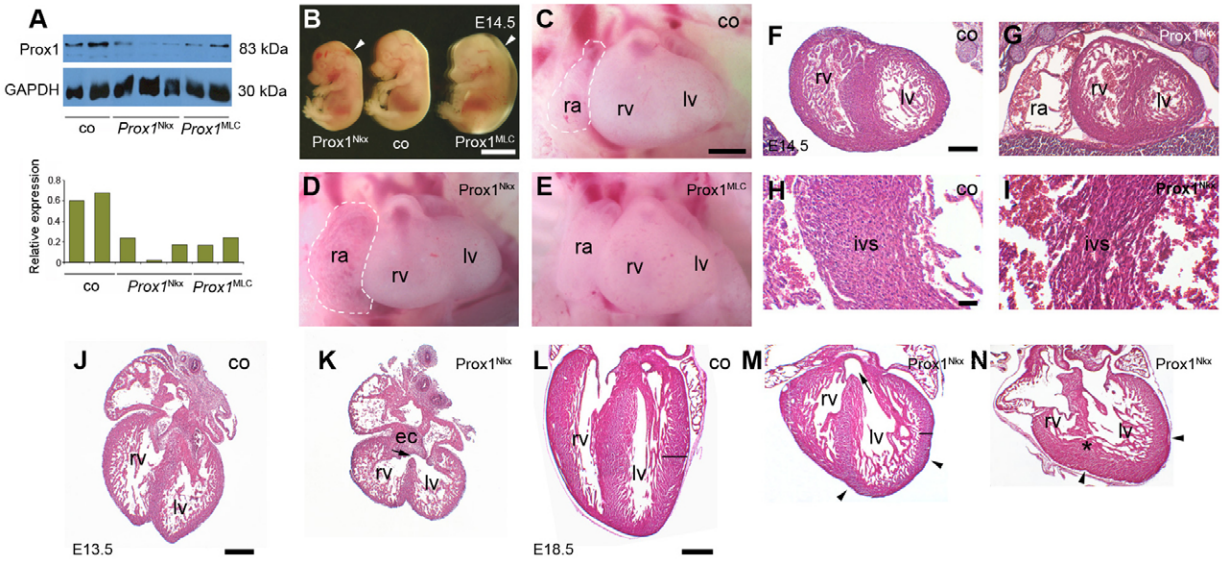

Fig. 2. Cardiac-specific loss of *Prox1* perturbs embryonic and heart development. (**A**) Western blots of E13.5 control (co), *Prox1*^{Nkx} and *Prox1*^{MLC} individual isolated mouse heart lysates for Prox1 and Gapdh and (beneath) quantification of protein levels, as normalised to Gapdh, using scanning densitometry. (**B-N**) Bright-field whole-mount left lateral views of E14.5 *Prox1*^{Nkx}, *Prox1*^{MLC} and control (co) littermate embryos (B), and frontal views of hearts in control (C), *Prox1*^{Nkx} (D) and *Prox1*^{MLC} (E) embryos. Frontal sections through E14.5 control (F,H) and *Prox1*^{Nkx} (G,I) embryos, E13.5 isolated control (J) and *Prox1*^{Nkx} (K) hearts, and E18.5 isolated control (L) and *Prox1*^{Nkx} (M,N) hearts. Prox1 protein levels are reduced to around a third of control levels in *Prox1*-conditional hearts (see A). *Prox1*^{Nkx} mutants are small, with oedema and cranial haemorrhaging, and *Prox1*^{MLC} mutants reveal extensive oedema (B, arrowheads). *Prox1*^{Nkx} hearts are hypoplastic with dilation of the right atrium (white dashed lines in C,D; G), and *Prox1*^{MLC} hearts are hypoplastic with reduced left ventricular expansion (E). Sections through *Prox1*^{Nkx} hearts reveal myocardial disarray, particularly in the interventricular septum (H,I). By E18.5, *Prox1*^{Nkx} hearts are rounded in shape and smaller than control hearts, the ventricular wall surface is irregular (arrowheads in M,N) with reduced compaction (black lines in L,M) and there are muscular septal defects (asterisk in N). Also note the membranous ventricular septal defect in *Prox1*^{Nkx} hearts (arrow, K,M). lv, left ventricle; rv, right ventricle; ra, right atrium; ivs, interventricular septum; ec, endocardial cushion. Scale bars: 5 mm in B; 50 μm in C-G,J,K; 10 μm in H,I; 1 mm in L-N.

Whole-mount and histological sections of *Prox1*^{Nkx} and *Prox1*^{MLC} embryos were examined between E10.5 and E18.5. No phenotype was evident between E10.5 and E12.5 (not shown), despite expression of Prox1 in the heart at these stages. At E13.5 and E14.5, the *Prox1*^{Nkx}- and *Prox1*^{MLC}-conditional mutants recapitulated the cardiac phenotype of the conventional knockout embryos described above. *Prox1*^{Nkx} embryos were slightly growth restricted (on average 5% smaller) compared with control littermates, with cranial haemorrhaging. Both *Prox1*^{Nkx} and *Prox1*^{MLC} embryos had oedema of varying severity (Fig. 2B), indicative of inadequate cardiac function. The hearts of both *Prox1*-conditional mutants were up to 30% smaller than controls hearts (Fig. 2C-E). Furthermore, in *Prox1*^{Nkx} hearts, the right atrium was reproducibly expanded (up to 2-fold) and blood-filled, never appearing to empty appropriately, irrespective of fixation stage during the cardiac cycle, suggesting that there might be impaired blood flow through the heart (Fig. 2D). Moreover, in the *Prox1*^{MLC} hearts, there was reduced expansion of the left ventricle (25% reduction in chamber size) consistent with haemodynamic obstruction (Fig. 2E). Haematoxylin and Eosin-stained frontal sections through E13.5 and E14.5 hearts (*Prox1*^{Nkx}, Fig. 2F-K; *Prox1*^{MLC}, not shown) revealed small thin-walled ventricles and disrupted myocardium with a highly disorganised interventricular septum (Fig. 2H,I). Additionally, membranous ventricular septal defects (VSDs) were observed in *Prox1*^{Nkx} embryos (Fig. 2J,K) that were unlikely to be due to myocardial disruption, but possibly related to additional endocardial cushion defects (not shown). By E18.5, the overall area of ventricular myocardium was significantly smaller in *Prox1*^{Nkx} than control hearts, in particular that of the right ventricle. Moreover, the myocardium was disorganised and less compacted (reduced by up to 50%) and the surface of the ventricles was irregular, although both compact and trabecular layers did appear to form (Fig. 2L-N). Consistent with the predominantly right-sided defects in *Prox1*^{Nkx} embryos, the pulmonary trunk was reduced in diameter, often being half the size of the aorta, suggesting impaired outflow tract remodelling. At E18.5, the membranous VSD was still evident in *Prox1*^{Nkx} embryos, and we also observed muscular VSDs (Fig. 2N) that were likely to result from the reduced level of myocardial compaction in the ventricles.

We observed variable and incomplete levels of *Prox1* deletion in the developing heart (Fig. 2A), which may be attributed to the mosaic nature of Cre expression as previously described for the Nkx2.5^{Cre}KI and MLC2v^{Cre}KI strains (Smart et al., 2007). Analysis of both *Prox1*^{Nkx} and *Prox1*^{MLC} mutant hearts confirmed specificity of phenotype at the level of the myocardium, as supported by immunostaining for markers of vascular endothelial and smooth muscle cells (Pecam1 and smooth muscle α-actin, respectively) that revealed normal coronary vessel development (see Fig. S3A-D in the supplementary material). Owing to the similarities in myocardial phenotype observed in both models, the term *Prox1*-conditional will be used to describe both the *Prox1*^{Nkx} and *Prox1*^{MLC} hearts unless specifically stated otherwise.

Sarcomeric integrity is disrupted in *Prox1*-conditional hearts

At a gross level, as determined by low-resolution histological analyses, loss of Prox1 function in the heart appeared to lead to myocardial disarray that was manifested in disorganisation of the

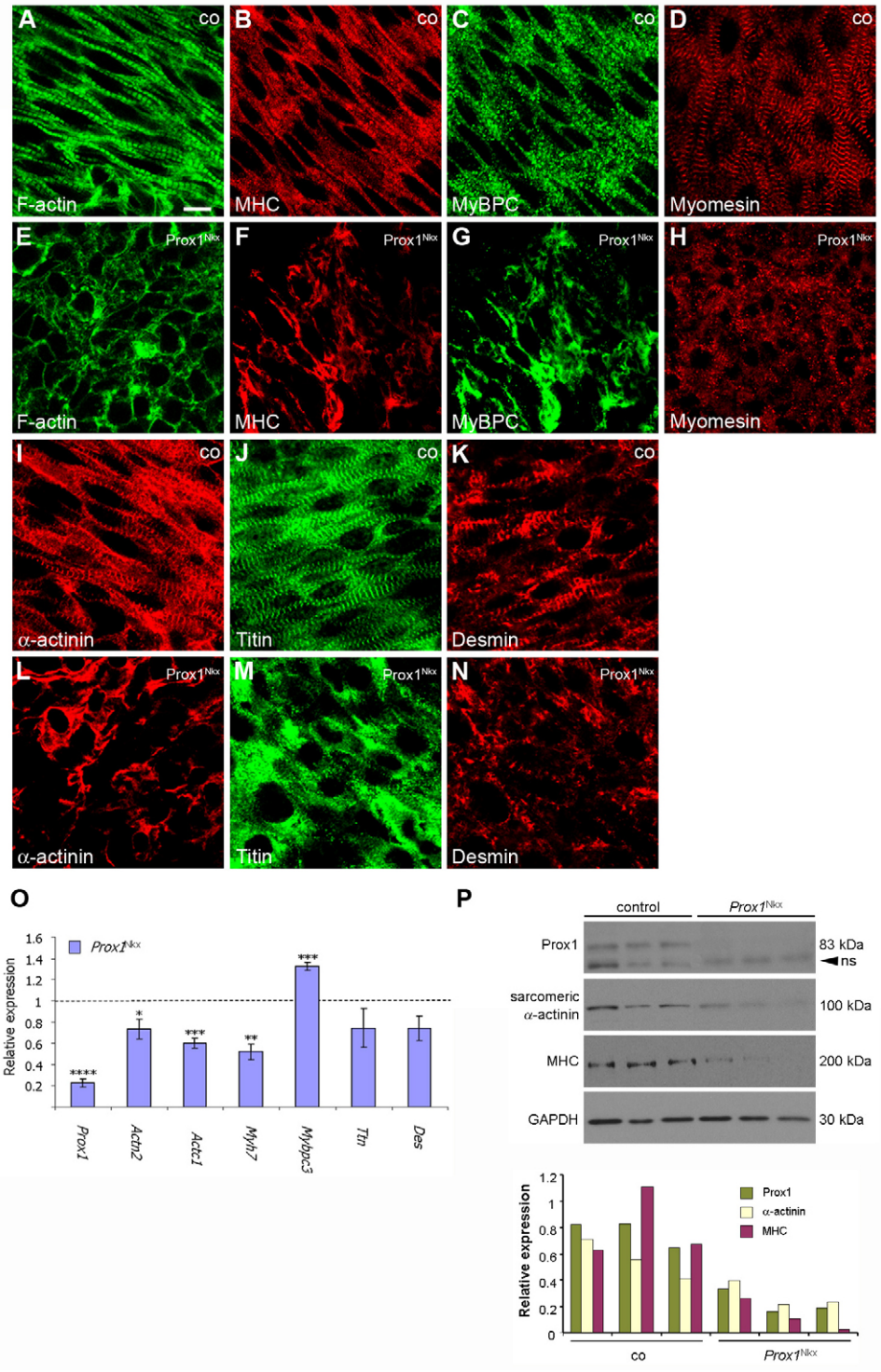

Fig. 3. All structural components of the sarcomere are severely disrupted in *Prox1*-conditional myocardium. (**A-N**) Confocal sections of immunostained E13.5 whole-mount hearts from control (co; A-D,I-K) and *Prox1*^{Nkx} (E-H,L-N) mouse embryos. Actin thin filaments and myosin thick filaments lack organisation and are not striated in *Prox1*-conditional hearts, as visualised by phalloidin staining (green; compare E with A) and immunostaining for sarcomeric myosin heavy chain (MHC) (red; B,F), respectively. Immunostaining for the thick filament component sarcomeric and cardiac myosin binding protein C (MyBP-C) further demonstrates thick filament disorganisation (green; C,G). M-band disruption is demonstrated by immunostaining for myomesin (red; D,H). Z-disc disruption in *Prox1*^{Nkx} hearts is revealed by immunostaining for sarcomeric α-actinin (red; I,L), titin N-terminus (green; J,M) and desmin (red; K,N). (**O**) Quantitative real-time PCR (qRT-PCR) for sarcomere component genes on E12.5 *Prox1*^{Nkx} hearts. Data are presented as mean ± s.e.m.; **P*<0.05, ***P*<0.003, ****P*<0.001, *****P*<9×10^{-7}. (**P**) Western blots of E13.5 control and *Prox1*^{Nkx} individual (half) heart lysates for Prox1 [non-specific (ns) band indicated by arrowhead], sarcomeric α-actinin, sarcomeric MHC and Gapdh, and quantification of protein levels, as normalised to Gapdh, using scanning densitometry. Scale bar: 10 μm.

myofibrils. To investigate this in more detail, the expression and localisation of sarcomeric markers was analysed by high-resolution confocal microscopy following immunostaining of whole-mount embryonic hearts. The relative distribution of the major components of the sarcomere is illustrated in Fig. S4A (see Fig. S4A in the supplementary material). In the first instance, colocalisation of Prox1 and selected sarcomeric markers (actin and sarcomeric α-actinin) was confirmed in E13.5 control hearts (see Fig. S1A-D in the supplementary material). *Prox1*-conditional E13.5 and E14.5 whole-mount hearts were stained with phalloidin to visualise F-actin and the arrangement of the thin filaments, and immunostained with antibodies to sarcomeric myosin heavy chain (MHC) and cardiac myosin binding protein C (MyBP-C) to visualise the thick filament architecture. Additionally, hearts were immunostained with antibodies to sarcomeric α-actinin, a crucial Z-disc protein that cross-links sarcomeric actin and is involved in many signalling transduction pathways, to myomesin, which localises to the M-band where it interacts with myosin and titin providing elasticity and stability to the sarcomere, and to β-catenin, which localises to the adherens junctions and demarcates cell-cell contacts (Fig. 3; see Fig.

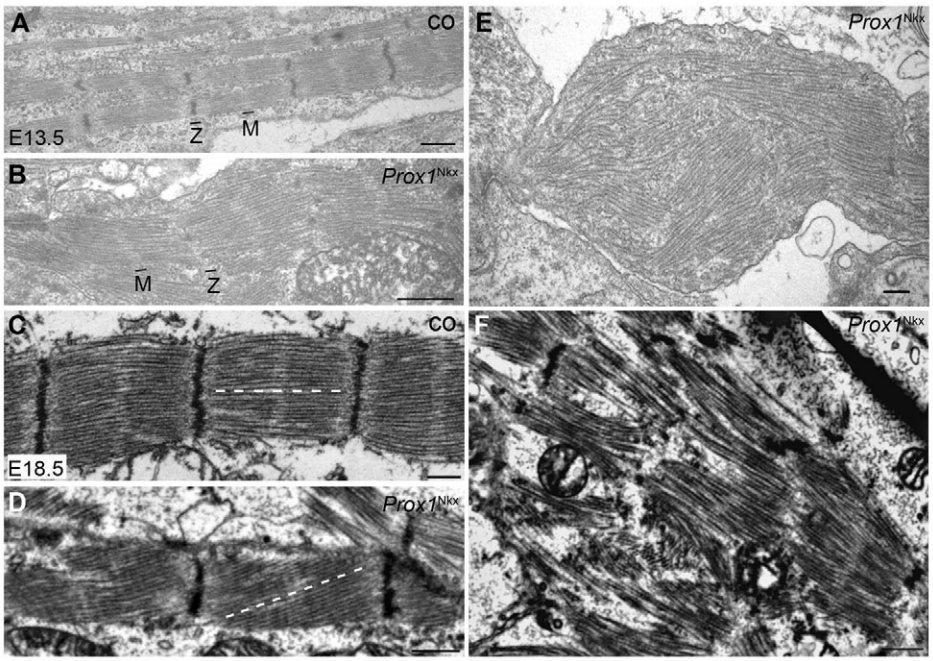

Fig. 4. Electron micrographs of muscle ultrastructure defects in *Prox1*-conditional myocardium.
(**A-F**) Transmission electron microscopy (TEM) on E13.5 (A,B,E) and E18.5 (C,D,F) control (co; A,C) and *Prox1*^{Nkx} (B,D,E,F) mouse hearts confirms the sarcomeric disruption in *Prox1*^{Nkx} ventricular myocardium. Note that C and D are in the same orientation and plane of section. There can be a complete loss of Z-disc (Z) material and intact M-band (M) (A), an accompanying disruption of the M-band (B), or disruption to the thick and thin filament alignment (dashed lines; C,D), associated with Z-disc disorganisation, whereas in the most severely affected hearts TEM reveals complete myofibril disarray (E,F). Scale bars: 500 nm.

S4A and Fig. S5A-F in the supplementary material). In *Prox1*-conditional hearts at E13.5, we consistently observed severe global disruption of thin filament, thick filament, Z-disc and M-band organisation in the ventricular myocardium as compared with littermate controls (Fig. 3A-I,L). Variation in the severity of disruption of actin filaments and α-actinin was evident (see Fig. S6 in the supplementary material), consistent with mosaicism in the level of *Prox1* knockdown (Fig. 2A; a western analysis for Prox1 expression with scanning densitometry normalised to Gapdh). We classified overall phenotype severity based on the following three criteria as revealed by the confocal ultrastructure analysis: (1) cardiomyocyte cell shape (using ImageJ, see Materials and methods), (2) sarcomeric striation and (3) myofibrillar organisation/cell alignment. Defects in one of these categories were classed as mild, of which we recorded 14.3% of *Prox1*^{Nkx} (n=56) and 18.2% of *Prox1*^{MLC} (n=41) mutants; defects in all three criteria were classed as severe, of which we recorded 85.7% of *Prox1*^{Nkx} (n=56) and 81.8% of *Prox1*^{MLC} (n=41) mutants at E13.5. Despite variation in the severity of the phenotype, the nature of the specific defects common to both the *Prox1*^{Nkx} and *Prox1*^{MLC} mutants, presented as anomalies in muscle ultrastructure, confirmed a cardiomyocyte-autonomous role for Prox1. The severe phenotype was incompatible with embryonic survival, whereas incomplete deletion of *Prox1* resulting in the mild phenotype contributed to a low incidence of survival of *Prox1*-conditional mutants to post-natal stages (5/111 *Prox1*^{Nkx} and 0/64 *Prox1*^{MLC}). Additionally, we occasionally observed thin filament and Z-disc disruption and loss of striation in *Prox1*^{Nkx} atrial myocardium (not shown), which is consistent with the expression patterns of *Prox1* and *Nkx2.5*.

To specifically evaluate Z-disc integrity in *Prox1*-conditional hearts, we immunostained for the titin N-terminus and desmin. Titin is a giant protein that spans half the width of a sarcomere, with its C-terminus localised at the M-band and its N-terminus at the Z-disc, where it interacts with sarcomeric α-actinin. Desmin is an intermediate filament protein that also interacts with sarcomeric α-actinin at Z-discs, providing a lateral connection between Z-discs of adjacent myofibrils (see Fig. S4A in the supplementary material). *Prox1*-conditional E13.5 hearts were triple stained for titin (Fig. 3J,M), desmin (Fig. 3K,N) and phalloidin (not shown), which demonstrated that loss of Prox1 results in a severe disruption of Z-disc organisation. The full extent of sarcomeric protein misregulation in *Prox1*-conditional hearts is summarised in Fig. S4B (see Fig. S4B in the supplementary material).

Given that Prox1 is a transcription factor, we sought to determine whether alterations in the expression levels of myofibril and Z-disc components might underlie the ultrastructure defects. E12.5 or E13.5 *Prox1*-conditional and control individual hearts were examined by quantitative real-time (qRT)-PCR or western blotting, respectively. qRT-PCR was carried out for genes encoding the sarcomere components that were shown to be mislocalised in *Prox1*-conditional myocardium. α-cardiac actin (*Actc1*), sarcomeric α-actinin (*Actn2*) and β-MHC (*Myh7*) were significantly downregulated and MyBP-C (*Mybpc3*) was significantly upregulated (Fig. 3O). Titin (*Ttn*) and desmin (*Des*) were consistently downregulated, but to varying levels, which led to the changes not being statistically significant (Fig. 3O). Nonetheless, these results confirm the extensive sarcomere dysgenesis in the *Prox1*-conditional mutant hearts both in terms of appropriate myofibril organisation and gene expression. Additionally, we analysed sarcomere component protein levels in E13.5 individual hearts. In accordance with the changes in gene expression, sarcomeric α-actinin and sarcomeric MHC were downregulated in *Prox1*-conditional hearts (Fig. 3P). Levels of desmin, β-catenin and vinculin were unchanged (not shown), which, alongside confocal immunofluorescence for β-catenin (see Fig. S5A-F in the supplementary material), confirmed that cell-cell contacts through adherens-type junctions were unaltered between neighbouring *Prox1*-conditional cardiomyocytes.

Subsequently, we examined the relationship between the level of Prox1 reduction and α-actinin expression further. Individual heart samples were analysed by both western blotting and immunostaining and we observed a direct correlation between the degree of Prox1 knockdown and the reduction in sarcomeric α-actinin levels (Fig. 3O,P). This suggests that Prox1 activity might regulate the expression of sarcomeric α-actinin and, moreover, that a modest yet significant reduction (0.7-fold) in α-actinin is sufficient to contribute to the myofibrillar disarray in the conditional mutant hearts (Fig. 3I,L).

Furthermore, this analysis demonstrated a definitive association between the level of Prox1 expression and the severity of the myocardial phenotype (Fig. 3O,P; see Fig. S6 in the supplementary material).

Sarcomere ultrastructure disruption was examined at higher resolution by transmission electron microscopy (TEM) in E13.5 and E18.5 *Prox1*^{Nkx} myocardium. At both developmental stages we observed variation in the severity of sarcomere ultrastructure defects in the *Prox1*^{Nkx} ventricular myocardium (Fig. 4A-F). Z-disc material was either entirely absent (Fig. 4B) or relatively dense but inappropriately organised (Fig. 4D). There was also an associated misalignment of the M-bands, with thick and thin filament disarray, suggesting that reduced Prox1 function impacts globally on sarcomeric organisation (Fig. 4D; see Discussion). Further examination of the cell-cell contacts, as a possible source of disruption to the muscle ultrastructure, revealed both intact adherens-type junctions (see Fig. S5G,H in the supplementary material), consistent with the β-catenin immunofluorescence data (see Fig. S5A-F in the supplementary material), and intact desmosomes (see Fig. S5I,J in the supplementary material) in the *Prox1*-conditional mutant hearts. Despite phenotypic variation, in the most severely affected cases we consistently observed a total lack of sarcomeric organisation at both E13.5 and E18.5 (Fig. 4E,F). Therefore, in combination, the confocal and TEM studies implicate Prox1 in organising components of the sarcomere and, furthermore, suggest that Prox1 is involved in maintaining myofibril ultrastructure throughout cardiogenesis.

Prox1 is essential for physiological foetal hypertrophy

We next investigated whether Prox1 plays a role in either the initial stages of myofibrillogenesis or in the maintenance of appropriate myofibril structure throughout later stages of cardiac development. To this end, we immunostained whole-mount *Prox1*-conditional hearts at E10.5, E11.5 and E12.5 for sarcomeric α-actinin and phalloidin to pinpoint exactly when the myocardial defects first arise. In the *Prox1*^{Nkx} mutants, *Prox1* levels were reduced from early cardiac crescent stages (E7.5) (Moses et al., 2001) onwards, and yet at E10.5 and E11.5 there was no sarcomeric disruption and the myofibrils appeared to have assembled correctly (Fig. 5A,D), whereas by E12.5 the first signs of myofibril disorganisation were observed (see Fig. S7A-D in the supplementary material). The fact that sarcomere defects do not manifest until E13.5 and then persist throughout the rest of development suggests that Prox1 is not required for the initiation of myofibrillogenesis but for the subsequent maintenance of appropriate sarcomeric structure and stability. In addition, we observed that in E13.5 *Prox1*-conditional hearts cardiomyocyte morphology and distribution were noticeably altered: the cardiomyocytes were more rounded in shape, disorganised and distributed in an apparently random pattern as compared with the control hearts, in which the cardiomyocytes had begun to elongate and align in parallel (Fig. 3A-N). Consistent with this, we observed a significant increase in α-actinin expression in wild-type hearts between E9.5 and E12.5, indicative of a requirement for sarcomeric-dependent cell growth after the recruitment of cells and at the onset of physiological hypertrophy (see Fig. S7E in the supplementary material). When sections of E18.5 *Prox1*-conditional and control hearts were examined by phalloidin staining and immunostaining for sarcomeric α-actinin we observed that a large proportion of cardiomyocytes were still rounded at E18.5, having failed to undergo hypertrophic growth and acquire the characteristic rod shape of mature cardiomyocytes (Fig. 5C,F).

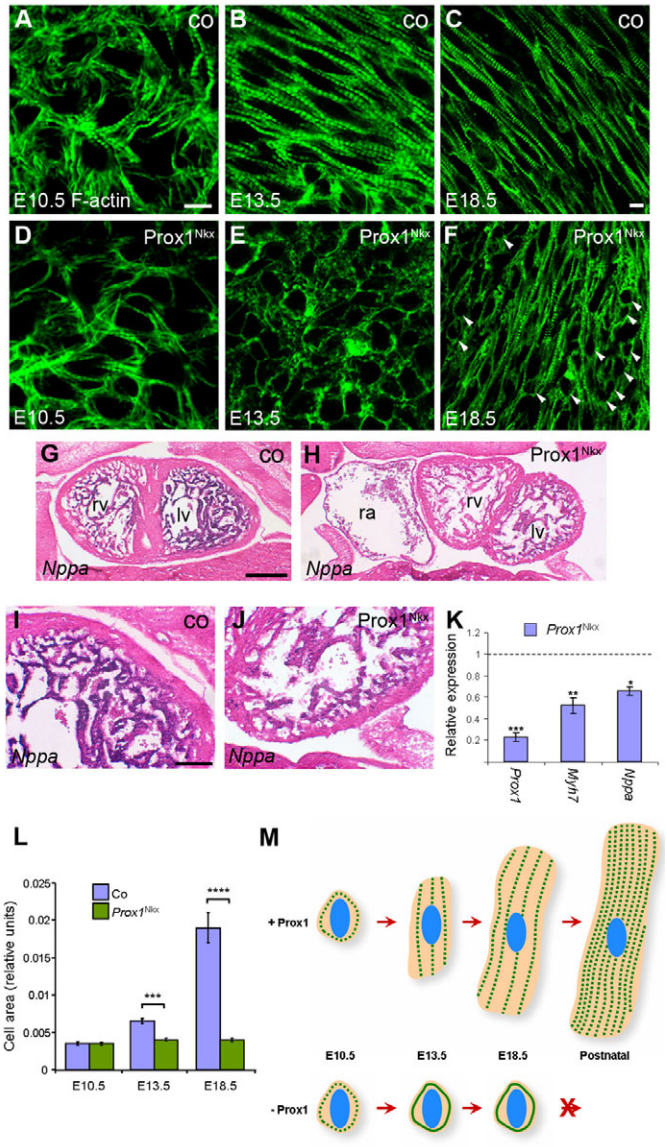

Fig. 5. Prox1 is required for foetal cardiomyocyte hypertrophy. (**A-F**) Phalloidin staining on E10.5 (A,D), E13.5 (B,E) and E18.5 (C,F) control (co; A-C) and *Prox1*^{Nkx} (D-F) whole-mount (A,B,D,E) and sections through (C,F) isolated mouse hearts. At E10.5, *Prox1*^{Nkx} cardiomyocytes are developing normally and the appropriate ultrastructure is laid down (A,D). From E13.5 onwards, *Prox1*^{Nkx} cardiomyocytes remain as small rounded cells that do not acquire the characteristic rod shape (arrowheads; E,F). (**G-J**) In situ hybridisation for *Nppa* transcripts on frontal sections of E13.5 control (G,I) and *Prox1*^{Nkx} (H,J) embryos. There is greatly reduced *Nppa* expression in *Prox1*^{Nkx} myocardium (H,J). lv, left ventricle; rv, right ventricle; ra, right atrium. (**K**) The reduced *Nppa* expression in *Prox1*^{Nkx} myocardium is confirmed by qRT-PCR on E12.5 isolated hearts. β-MHC (*Myh7*) was also found to be downregulated. (**L**) Morphometric analysis of cell shape (using ImageJ) confirmed a lack of increase in cell size because of impaired elongation and hypertrophic growth in *Prox1*^{Nkx} cardiomyocytes during development, excluding the possibility that the rounded cells simply reflect an alteration in cell shape. In K,L, mean ± s.e.m.; $*P<0.001$, $**P<0.003$, $***P<9\times10^{-7}$ (K), $***P<7\times10^{-8}$ (L), $****P<3\times10^{-12}$. (**M**) Foetal cardiomyocyte hypertrophic growth throughout normal development and in the absence of Prox1, where sarcomere striation is lost, myofibrils do not align and cardiomyocytes do not grow by hypertrophy. Green dotted lines, striated myofibrils; solid green lines, failed striation; blue ovals, nuclei. Scale bars: 10 μm in A-F; 50 μm in G,H; 20 μm in I,J.

Hypertrophy in adult hearts is induced by a large variety of stimuli, but the consistent end point is re-expression of a foetal gene programme, including *Nppa* (Anf), *Myh7* (β-MHC) and *Nppb* (BNP) (Molkentin et al., 1998). During development, *Nppa*, *Myh7* and *Nppb* are markers of myocardial differentiation and chamber expansion, but because differentiation per se is accompanied by a concomitant increase in cardiomyocyte cell growth, we examined the expression levels of *Nppa* and *Myh7* as surrogate markers of foetal hypertrophy. qRT-PCR on E12.5 hearts and in situ hybridisation on E13.5 embryo sections revealed that both genes were significantly downregulated in *Prox1*^{Nkx} hearts (Fig. 5G-K), not only indicating that was there markedly reduced foetal hypertrophic growth in the absence of Prox1, but also suggesting that *Prox1*-conditional hearts are not hypoplastic, but hypotrophic. Morphometric measurements of cell size revealed that cardiomyocytes in *Prox1*^{Nkx} hearts failed to enlarge during development, confirming a defect in hypertrophic growth as opposed to an alteration in cell shape (Fig. 5L). Immunostaining for phosphohistone H3, a marker of cells in mitosis, and TUNEL assays confirmed that there was no decrease in proliferation or increase in apoptosis between E10.5 and E13.5 (see Fig. S8 in the supplementary material). Therefore, in the absence of Prox1, although laid down appropriately in early heart development, the sarcomere structure is not maintained, resulting in myofibril disruption, loss of striation and a failure of cardiomyocyte hypertrophic growth and maturation (Fig. 5M).

Prox1 directly regulates fundamental components of the sarcomere

To gain specific insight into the molecular mechanism(s) by which Prox1 regulates myofibril organisation we sought to identify direct downstream targets of Prox1 in the developing heart. Until now, no in vivo target of Prox1 has been identified, nor has a definitive consensus Prox1 DNA-binding site been determined. Therefore, we combined chromatin immunoprecipitation (ChIP) against endogenous Prox1 with microarray analysis (ChIP-on-chip). ChIP-on-chip revealed putative Prox1-bound enhancer regions of genes encoding the Z-disc protein α-actinin (*Actn2*) and the myofibrillar and adherens junction proteins N-RAP (*Nrap*) and zyxin (*Zyx*), both of which directly interact with α-actinin in the Z-disc (Fig. 6A). ChIP of the three enhancer elements was confirmed by PCR (see Fig. S9A in the supplementary material). We analysed the *Actn2*, *Nrap* and *Zyx* target sequences for predicted transcription factor binding sites using MatInspector Professional (http://www.genomatix.de): 40-50 transcription factor binding sites were predicted per sequence but no putative Prox1 or Prospero (the *Drosophila* homologue of Prox1) binding sites were identified, although the Prox1 sites described to date are highly degenerate and predicted based on a Prospero consensus (Cook et al., 2003; Lengler et al., 2005; Shin et al., 2006). The lack of a core consensus motif within the three Prox1-bound enhancer elements identified for *Actn2*, *Nrap* and *Zyx*, despite the conservation of each element across species, is consistent with results obtained from unbiased screens of genome-wide conserved regulatory sequence variants (Pennacchio et al., 2006).

The ChIP data were subsequently validated by EMSAs with overlapping probes from each of the three enhancer regions and in vitro translated Prox1 or lysates from mouse P19Cl6 cells overexpressing Prox1 (see Fig. S9B-D in the supplementary material). Competition gel shifts with unlabelled probe (Fig. 6B) and antibody supershifts (Fig. 6C) of the refined oligonucleotide sequences (60 bp) confirmed specific Prox1 binding to the enhancers within *Actn2*, *Nrap* and *Zyx*. Prox1-induced transcription via all three enhancer elements was demonstrated by cotransfection and reporter gene activation assays (*Actn2*, 15-fold activation; *Nrap*, 32-fold; *Zyx*, 9-fold) (Fig. 6D). qRT-PCR for *Nrap* and *Zyx* (Fig. 6E) confirmed reduced expression of these factors in a *Prox1*-deficient background, as was previously determined for *Actn2* (Fig. 3O).

DISCUSSION

The failure of *Prox1*-conditional cardiomyocytes to grow and to maintain sarcomere organisation throughout development results in hypotrophic hearts that are insufficient to sustain life beyond birth. We observed disruption of the sarcomere at the level of both gene expression and protein localisation and have identified Prox1-bound enhancer elements for key sarcomere-associated genes, indicating that Prox1 regulates myofibrillar organisation both directly in terms of protein expression, and indirectly via intermediate factors that control sarcomere protein localisation and integration.

Prox1 deficiency impacts directly on sarcomeric components that facilitate Z-disc and thin filament interaction. Reduced expression of *Nrap* and *Zyx* in *Prox1*-conditional hearts, two genes that are direct transcriptional targets of Prox1, is highly significant in terms of maintaining Z-disc stability. N-RAP has been proposed to act as a catalytic scaffold for the association of thin filament actin and Z-disc α-actinin during myofibrillogenesis (Dhume et al., 2006), and zyxin also interacts with α-actinin to facilitate actin assembly and organisation (Crawford et al., 1992; Frank et al., 2006). During myofibrillogenesis, N-RAP and zyxin are associated with cell-cell contacts that make up the developing intercalated discs, which ultimately mature during post-natal stages (Perriard et al., 2003). Our confocal and TEM observations that cell junctions (β-catenin-positive adherens-type junctions and desmosomes) are appropriately established and remain intact between neighbouring cardiomyocytes in *Prox1*-conditional mutants, suggest that the role of Prox1 is primarily to regulate *Nrap* and *Zyx* to facilitate cross-linking between actin and α-actinin in the Z-disc as one of the fundamental associations of the sarcomere (see Fig. S4A in the supplementary material). *Actn2* is also implicated in this study as a direct target of Prox1, and the modest, yet significant, reduction in the expression levels of *Actn2* in a *Prox1* mutant background, correlating with the Z-disc disruption, underlines the crucial role of α-actinin in maintaining sarcomere integrity. Moreover, as *Zyx*-null mice are viable (Hoffman et al., 2003), although their hearts have not been examined in detail for histological defects, the phenotype we describe represents a cumulative effect on the actin–α-actinin interaction: directly, via α-actinin expression and localisation, and through interactions with the co-factors N-RAP and zyxin.

Perturbation of the actin–α-actinin association directly explains the Z-disc anomalies in *Prox1*-null hearts. Although we cannot entirely exclude additional effects of loss of Prox1 function, normal levels of cardiomyocyte proliferation and apoptosis and the specificity of phenotype at the level of sarcomeric maintenance suggest that the latter is the primary defect in *Prox1*-conditional mutants. Moreover, thin filament–Z-disc disruption will feedback directly onto the thin and thick filament arrangement of the sarcomere, as observed at the level of TEM, resulting in a more global disorganisation of myofibrils (see Fig. S4B in the supplementary material). The latter might also explain the observed M-band defects, but equally these might relate more directly to misregulation of *Nrap* in the *Prox1*-mutant background, as N-RAP associates with the M-bands of maturing myofibrils where it acts as a catalytic scaffold (Lu et al., 2005).

Prox1 is not required for the initial stages of myofibrillogenesis because the phenotypic defects do not begin to manifest until E12.5. Sarcomere proteins are expressed immediately prior to the onset of

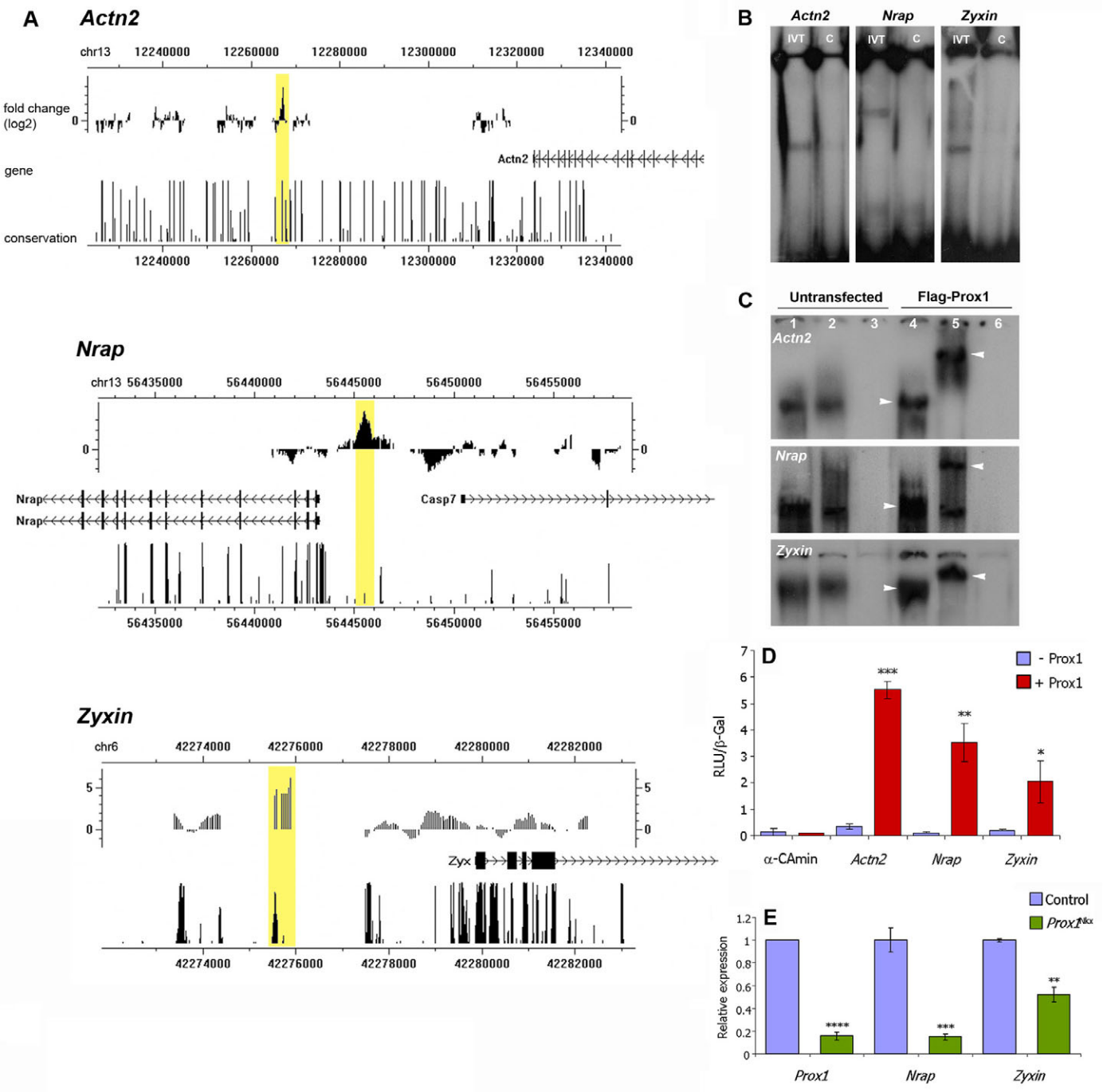

Fig. 6. Prox1 directly regulates the genes encoding the structural proteins α-actinin, N-RAP and zyxin. (**A**) The sarcomere and sarcomere-related protein genes *Actn2* (sarcomeric α-actinin), *Nrap* and *Zyx* were identified as potential downstream targets of Prox1 by ChIP-on-chip. For each locus, the genomic region immunoprecipitated by anti-Prox1 is indicated by a yellow box, the closest gene is labelled and the degree of conservation shown. Conservation patterns are based on phastCons scores (http://genome.ucsc.edu). (**B**) EMSAs with in vitro translated (IVT) Prox1 and ^{32}P-labelled oligonucleotides (60 bp) identified from each of the *Actn2*, *Nrap* and *Zyx* putative Prox1-bound elements (see Fig. S9 in the supplementary material) isolated via the ChIP-on-chip shown in A. A 10-fold excess of unlabelled oligonucleotide was used in competitive assays as evidence of specific binding (lanes C). (**C**) EMSAs with nuclear extracts from mouse P19Cl6 cell lysates either untransfected (lanes 1-3) or transfected with Flag-Prox1 (lanes 4-6) and ^{32}P-labelled elements as in B. Lanes 1 and 4 are lysate alone, lanes 2 and 5 are lysate plus an anti-Flag antibody, and lanes 3 and 6 are anti-Flag-alone controls. Note the evidence of a supershift in lane 5 compared with lane 4 for each of the *Actn2*, *Nrap* and *Zyx* elements (arrowheads), which is indicative of specific binding by Flag-Prox1. The presence of a comparatively weak band in lanes 1 and 2 in each case represents binding by endogenous Prox1, which is expressed in P19Cl6 cells (data not shown). (**D**) In vitro transcription assays demonstrate Prox1 transactivation of a luciferase reporter downstream of the *Actn2*, *Nrap* and *Zyx* putative Prox1-binding elements and minimal reporter. Note the significant activation by Prox1 of the *Actn2*, *Nrap* and *Zyx* reporters. (**E**) qRT-PCR for *Nrap* and *Zyx* confirms reduced expression of these factors in a *Prox1*-deficient background, as was previously determined for *Actn2* (see Fig. 3O). In D,E, data are presented as mean ± s.e.m.; **P*<0.05, ***P*<0.001, ****P*<0.003, *****P*<9×10^{-7}.

beating and, once integrated into mature myofibrils, they tend to have a relatively long half-life that varies between 3 and 10 days (Martin, 1981). Moreover, between E8.25 and E10.5, the developing heart increases in mass primarily through the addition of cells from the second cardiac lineage (Zaffran et al., 2004). Therefore, there may be little requirement for newly synthesised structural proteins during these early stages of heart development. The initial activation of the genes encoding sarcomeric proteins is clearly carried out by alternate, as yet unidentified, transcriptional regulation pathways, with the role of Prox1 confined to regulating sarcomere maintenance and stability from E10.5 onwards, when all populations of cardiac cells have been acquired and the developing heart continues to grow by a combination of both cardiomyocyte hyperplasia and hypertrophy. The fact that we observed significantly impaired hypertrophic growth following loss of *Prox1* is secondary to the primary defect of disrupted assembly of sarcomere proteins. Developing cardiomyocytes elongate in a unidirectional manner by addition of sarcomeres to the existing myofibrils, the timing of which corresponds precisely with the onset of myocardial disruption and failure of the cells to elongate in *Prox1*-conditional myocardium (see the model in Fig. 5M).

In conclusion, Prox1 is essential for the maintenance and maturation of the sarcomere in developing cardiomyocytes, which in turn are crucial for hypertrophic growth and maturation of the embryonic myocardium. The identification of the genes encoding the structural proteins α-actinin, N-RAP and zyxin, as direct targets of Prox1 suggests that misregulation of essential sarcomere components and their interacting protein partners is the primary cause of myofibril disruption in *Prox1*-conditional myocardium. A number of other studies have described roles for transcription factors in initiating or maintaining cardiac muscle ultrastructure during development and disease, most notably serum response factor (Srf) (Balza and Misra, 2006; Nelson et al., 2005), Gata4, Nkx2.5 and Mef2 (Akazawa and Komuro, 2003) and calcineurin (Ppp3ca)/Nfat (Bourajjaj et al., 2008; Heineke and Molkentin, 2006). However, to the best of our knowledge, no study to date has demonstrated direct transcriptional regulation of structural protein genes in vivo.

Aberrant terminal differentiation and improper assembly of contractile protein filaments are associated with a number of cardiac myopathies (Engel, 1999; Gregorio and Antin, 2000; Seidman and Seidman, 2001). Many of these disorders are caused by mutations in components of the myofibrillar apparatus itself, including β-MHC, troponins T and I, titin and α-tropomyosin (Alcalai et al., 2008; Chang and Potter, 2005), or perturbations in the associated calcium-dependent signalling pathways (Frey et al., 2004; Molkentin et al., 1998). However, a large proportion of cardiomyopathies remain unexplained, with no mutations found in sarcomere or sarcomere-related proteins. Our study not only provides novel insight into the transcriptional regulation of cardiomyocyte ultrastructure and hypertrophy during development, but also implicates Prox1 as a crucial regulatory factor that might underlie the pathology of both inherited and acquired myopathic disease.

We thank K. Venner for technical assistance with electron microscopy, A. Cook for advice on E18.5 heart analysis, C. Shang for advice on the ChIP protocol, D. Kelberman for advice on the EMSA protocol, and D. Fürst (titin and α-actinin) and T. Obinata (MyBP-C) for antibodies. This work was funded by the British Heart Foundation, the Medical Research Council, and by R01-HL073402 (G.O.) from the National Institutes of Health and by the American Lebanese Syrian Associated Charities (ALSAC). Deposited in PMC for release after 12 months.

Supplementary material

Supplementary material for this article is available at http://dev.biologists.org/cgi/content/full/136/3/495/DC1

References

Ahuja, P., Perriard, E., Perriard, J. C. and Ehler, E. (2004). Sequential myofibrillar breakdown accompanies mitotic division of mammalian cardiomyocytes. *J. Cell Sci.* **117**, 3295-3306.

Akazawa, H. and Komuro, I. (2003). Roles of cardiac transcription factors in cardiac hypertrophy. *Circ. Res.* **92**, 1079-1088.

Alcalai, R., Seidman, J. G. and Seidman, C. E. (2008). Genetic basis of hypertrophic cardiomyopathy: from bench to the clinics. *J. Cardiovasc. Electrophysiol.* **19**, 104-110.

Angelo, S., Lohr, J., Lee, K. H., Ticho, B. S., Breitbart, R. E., Hill, S., Yost, H. J. and Srivastava, D. (2000). Conservation of sequence and expression of Xenopus and zebrafish dHAND during cardiac, branchial arch and lateral mesoderm development. *Mech. Dev.* **95**, 231-237.

Balza, R. O., Jr and Misra, R. P. (2006). Role of the serum response factor in regulating contractile apparatus gene expression and sarcomeric integrity in cardiomyocytes. *J. Biol. Chem.* **281**, 6498-6510.

Bourajjaj, M., Armand, A. S., da Costa Martins, P. A., Weijts, B., van der, N. R., Heeneman, S., Wehrens, X. H. and De Windt, L. J. (2008). NFATc2 is a necessary mediator of calcineurin-dependent cardiac hypertrophy and heart failure. *J. Biol. Chem.* **283**, 22295-22303.

Chang, A. N. and Potter, J. D. (2005). Sarcomeric protein mutations in dilated cardiomyopathy. *Heart Fail. Rev.* **10**, 225-235.

Chen, J., Kubalak, S. W. and Chien, K. R. (1998). Ventricular muscle-restricted targeting of the RXRalpha gene reveals a non-cell-autonomous requirement in cardiac chamber morphogenesis. *Development* **125**, 1943-1949.

Cook, T., Pichaud, F., Sonneville, R., Papatsenko, D. and Desplan, C. (2003). Distinction between color photoreceptor cell fates is controlled by Prospero in Drosophila. *Dev. Cell* **4**, 853-864.

Crawford, A. W., Michelsen, J. W. and Beckerle, M. C. (1992). An interaction between zyxin and alpha-actinin. *J. Cell Biol.* **116**, 1381-1393.

Dhume, A., Lu, S. and Horowits, R. (2006). Targeted disruption of N-RAP gene function by RNA interference: a role for N-RAP in myofibril organization. *Cell Motil. Cytoskeleton* **63**, 493-511.

Dyer, M. A., Livesey, F. J., Cepko, C. L. and Oliver, G. (2003). Prox1 function controls progenitor cell proliferation and horizontal cell genesis in the mammalian retina. *Nat. Genet.* **34**, 53-58.

Dyson, E., Sucov, H. M., Kubalak, S. W., Schmid-Schonbein, G. W., DeLano, F. A., Evans, R. M., Ross, J., Jr and Chien, K. R. (1995). Atrial-like phenotype is associated with embryonic ventricular failure in retinoid X receptor alpha–/– mice. *Proc. Natl. Acad. Sci. USA* **92**, 7386-7390.

Ehler, E., Rothen, B. M., Hammerle, S. P., Komiyama, M. and Perriard, J. C. (1999). Myofibrillogenesis in the developing chicken heart: assembly of Z-disk, M-line and the thick filaments. *J. Cell Sci.* **112**, 1529-1539.

Engel, A. G. (1999). Myofibrillar myopathy. *Ann. Neurol.* **46**, 681-683.

Frank, D., Kuhn, C., Katus, H. A. and Frey, N. (2006). The sarcomeric Z-disc: a nodal point in signalling and disease. *J. Mol. Med.* **84**, 446-468.

Frey, N., Barrientos, T., Shelton, J. M., Frank, D., Rutten, H., Gehring, D., Kuhn, C., Lutz, M., Rothermel, B., Bassel-Duby, R. et al. (2004). Mice lacking calsarcin-1 are sensitized to calcineurin signaling and show accelerated cardiomyopathy in response to pathological biomechanical stress. *Nat. Med.* **10**, 1336-1343.

Gregorio, C. C. and Antin, P. B. (2000). To the heart of myofibril assembly. *Trends Cell Biol.* **10**, 355-362.

Habara-Ohkubo, A. (1996). Differentiation of beating cardiac muscle cells from a derivative of P19 embryonal carcinoma cells. *Cell Struct. Funct.* **21**, 101-110.

Harvey, N. L., Srinivasan, R. S., Dillard, M. E., Johnson, N. C., Witte, M. H., Boyd, K., Sleeman, M. W. and Oliver, G. (2005). Lymphatic vascular defects promoted by Prox1 haploinsufficiency cause adult-onset obesity. *Nat. Genet.* **37**, 1072-1081.

Heineke, J. and Molkentin, J. D. (2006). Regulation of cardiac hypertrophy by intracellular signalling pathways. *Nat. Rev. Mol. Cell Biol.* **7**, 589-600.

Hill, A. A. and Riley, P. R. (2004). Differential regulation of Hand1 homodimer and Hand1-E12 heterodimer activity by the cofactor FHL2. *Mol. Cell. Biol.* **24**, 9835-9847.

Hirschy, A., Schatzmann, F., Ehler, E. and Perriard, J. C. (2006). Establishment of cardiac cytoarchitecture in the developing mouse heart. *Dev. Biol.* **289**, 430-441.

Hoffman, L. M., Nix, D. A., Benson, B., Boot-Hanford, R., Gustafsson, E., Jamora, C., Menzies, A. S., Goh, K. L., Jensen, C. C., Gertler, F. B. et al. (2003). Targeted disruption of the murine zyxin gene. *Mol. Cell. Biol.* **23**, 70-79.

Kuo, C. T., Morrisey, E. E., Anandappa, R., Sigrist, K., Lu, M. M., Parmacek, M. S., Soudais, C. and Leiden, J. M. (1997). GATA4 transcription factor is required for ventral morphogenesis and heart tube formation. *Genes Dev.* **11**, 1048-1060.

Lengler, J., Bittner, T., Munster, D., Gawad, A. and Graw, J. (2005). Agonistic and antagonistic action of AP2, Msx2, Pax6, Prox1 AND Six3 in the regulation of Sox2 expression. *Ophthalmic Res.* **37**, 301-309.

Lu, S., Borst, D. E. and Horowits, R. (2005). N-RAP expression during mouse heart development. *Dev. Dyn.* **233**, 201-212.

Martin, A. F. (1981). Turnover of cardiac troponin subunits. Kinetic evidence for a precursor pool of troponin-I. *J. Biol. Chem.* **256**, 964-968.

McBurney, M. W., Jones-Villeneuve, E. M., Edwards, M. K. and Anderson, P. J. (1982). Control of muscle and neuronal differentiation in a cultured embryonal carcinoma cell line. *Nature* **299**, 165-167.
Molkentin, J. D., Lu, J. R., Antos, C. L., Markham, B., Richardson, J., Robbins, J., Grant, S. R. and Olson, E. N. (1998). A calcineurin-dependent transcriptional pathway for cardiac hypertrophy. *Cell* **93**, 215-228.
Moorman, A. F., Houweling, A. C., de Boer, P. A. and Christoffels, V. M. (2001). Sensitive nonradioactive detection of mRNA in tissue sections: novel application of the whole-mount in situ hybridization protocol. *J. Histochem. Cytochem.* **49**, 1-8.
Moses, K. A., DeMayo, F., Braun, R. M., Reecy, J. L. and Schwartz, R. J. (2001). Embryonic expression of an Nkx2-5/Cre gene using ROSA26 reporter mice. *Genesis* **31**, 176-180.
Nelson, T. J., Balza, R., Jr, Xiao, Q. and Misra, R. P. (2005). SRF-dependent gene expression in isolated cardiomyocytes: regulation of genes involved in cardiac hypertrophy. *J. Mol. Cell. Cardiol.* **39**, 479-489.
Oliver, G., Sosa-Pineda, B., Geisendorf, S., Spana, E. P., Doe, C. Q. and Gruss, P. (1993). Prox 1, a prospero-related homeobox gene expressed during mouse development. *Mech. Dev.* **44**, 3-16.
Peirson, S. N., Butler, J. N. and Foster, R. G. (2003). Experimental validation of novel and conventional approaches to quantitative real-time PCR data analysis. *Nucleic Acids Res.* **31**, e73.
Pennacchio, L. A., Ahituv, N., Moses, A. M., Prabhakar, S., Nobrega, M. A., Shoukry, M., Minovitsky, S., Dubchak, I., Holt, A., Lewis, K. D. et al. (2006). *In vivo* enhancer analysis of human conserved non-coding sequences. *Nature* **444**, 499-502.
Perriard, J. C., Hirschy, A. and Ehler, E. (2003). Dilated cardiomyopathy: a disease of the intercalated disc? *Trends Cardiovasc. Med.* **13**, 30-38.
Pyle, W. G. and Solaro, R. J. (2004). At the crossroads of myocardial signaling: the role of Z-discs in intracellular signaling and cardiac function. *Circ. Res.* **94**, 296-305.
Qin, J., Gao, D. M., Jiang, Q. F., Zhou, Q., Kong, Y. Y., Wang, Y. and Xie, Y. H. (2004). Prospero-related homeobox (Prox1) is a corepressor of human liver receptor homolog-1 and suppresses the transcription of the cholesterol 7-alpha-hydroxylase gene. *Mol. Endocrinol.* **18**, 2424-2439.
Rodriguez-Niedenfuhr, M., Papoutsi, M., Christ, B., Nicolaides, K. H., von Kaisenberg, C. S., Tomarev, S. I. and Wilting, J. (2001). Prox1 is a marker of ectodermal placodes, endodermal compartments, lymphatic endothelium and lymphangioblasts. *Anat. Embryol.* **204**, 399-406.
Seidman, J. G. and Seidman, C. (2001). The genetic basis for cardiomyopathy: from mutation identification to mechanistic paradigms. *Cell* **104**, 557-567.
Shin, J. W., Min, M., Larrieu-Lahargue, F., Canron, X., Kunstfeld, R., Nguyen, L., Henderson, J. E., Bikfalvi, A., Detmar, M. and Hong, Y. K. (2006). Prox1 promotes lineage-specific expression of fibroblast growth factor (FGF) receptor-3 in lymphatic endothelium: a role for FGF signaling in lymphangiogenesis. *Mol. Biol. Cell* **17**, 576-584.
Smart, N., Risebro, C. A., Melville, A. A., Moses, K., Schwartz, R. J., Chien, K. R. and Riley, P. R. (2007). Thymosin beta4 induces adult epicardial progenitor mobilization and neovascularization. *Nature* **445**, 177-182.
Sosa-Pineda, B., Wigle, J. T. and Oliver, G. (2000). Hepatocyte migration during liver development requires Prox1. *Nat. Genet.* **25**, 254-255.
Tomarev, S. I., Sundin, O., Banerjee-Basu, S., Duncan, M. K., Yang, J. M. and Piatigorsky, J. (1996). Chicken homeobox gene Prox 1 related to Drosophila prospero is expressed in the developing lens and retina. *Dev. Dyn.* **206**, 354-367.
Wigle, J. T. and Oliver, G. (1999). Prox1 function is required for the development of the murine lymphatic system. *Cell* **98**, 769-778.
Wigle, J. T., Chowdhury, K., Gruss, P. and Oliver, G. (1999). Prox1 function is crucial for mouse lens-fibre elongation. *Nat. Genet.* **21**, 318-322.
Zaffran, S., Kelly, R. G., Meilhac, S. M., Buckingham, M. E. and Brown, N. A. (2004). Right ventricular myocardium derives from the anterior heart field. *Circ. Res.* **95**, 261-268.